Available online at www.sciencedirect.com
SCIENCE DIRECT®
Solid State Sciences 5 (2003) 409–417
Solid State Sciences
www.elsevier.com/locate/ssscie

Reactivity of oxygen of complex cobaltates $La_{1-x}Sr_xCoO_{3-\delta}$ and $LaSrCoO_4$

Ludmila Borovskikh [a], Galina Mazo [a,*], Erhard Kemnitz [b]

[a] *Department of Chemistry, Lomonosov Moscow State University, Leninskie Gory, 119992, Moscow, Russia*
[b] *Institute of Chemistry, Humboldt University, Brook-Taylor Strasse 2, 12489 Berlin, Germany*

Received 23 September 2002; received in revised form 14 January 2003; accepted 15 January 2003

Abstract

Complex oxides $La_{1-x}Sr_xCoO_{3-\delta}$ ($x = 0.0$, 0.3, 0.5) with perovskite-like structure and $LaSrCoO_4$ with layered K_2NiF_4-type structure have been prepared using freeze-drying technique. The oxygen content of the single-phase samples was determined by iodometric titration. The oxygen mobility and catalytic activity of all cobaltate samples in the reaction of CH_4 oxidation were studied under dynamic-thermal ^{18}O-isotope exchange conditions. Catalytic reactions of CH_4 and CO oxidation have also been performed under steady flow conditions. The correlations between oxygen mobility and structural features of the catalyst and its initial oxygen deficiency has been established. $La_{0.5}Sr_{0.5}CoO_{2.92}$ and $La_{0.7}Sr_{0.3}CoO_{2.96}$ with deficiency in oxygen sublattice were more active in isotope exchange and catalysis, while $LaCoO_3$ and $LaSrCoO_4$ with the stoichiometric oxygen content demonstrated lower activity. The mobility of oxygen in layered $LaSrCoO_4$ is significantly higher than in $LaCoO_3$. Analysis of the methane oxidation using ^{18}O ^{18}O allowed to clarify the steps of the catalytic process. It was found also that methane is oxidized by the lattice oxygen of the catalyst.
© 2003 Éditions scientifiques et médicales Elsevier SAS. All rights reserved.

Keywords: Cobaltates; Oxygen nonstoichiometry; Oxygen mobility; ^{18}O-isotope exchange; Methane oxidation

1. Introduction

Among a variety of complex oxides ABO_3 perovskites (where A—rare earth or alkaline earth metal, B—transition metal) are of special interest due to their outstanding magnetic and transport properties as well as their ability to catalyze a large number of oxidation and reduction reactions [1–3], e.g.: total oxidation of CO and CH_4, oxidative coupling of methane, dehydrogenation of propane and reduction of NO_x. $LaCoO_3$ was shown to be one of the most active in oxidation processes [4].

The mobility of oxygen ions, directly related to the catalytic activity in oxidation reactions, depends on the concentration of oxygen vacancies, which can be modified by heterovalent doping. The ionic radius of Sr^{2+} is close to that one of La^{3+}, thus giving possibility to substitute La for Sr and to obtain a highly deficient oxygen sublattice and, hence, high oxygen mobility in $La_{1-x}Sr_xCoO_{3-\delta}$. Activity of substituted cobaltates in oxidation processes was proved to be higher than that of $LaCoO_3$ [5,6]. All oxygen sites in perovskite structure are practically the same (Fig. 1). Modification of the perovskite structure by introducing additional (La,Sr)O layer gives $La_{2-x}Sr_xCoO_{4\pm\delta}$ phases with K_2NiF_4-type structure with two different kinds of oxygen sites (Fig. 2). Calculation of bond valence parameters using the method proposed by Brown et al. [7] shows potentially higher oxygen mobility in $La_{2-x}Sr_xCoO_{4\pm\delta}$ compared to $La_{1-x}Sr_xCoO_{3-\delta}$. The catalytic behavior of layered $La_{2-x}Sr_xCoO_{4\pm\delta}$ in the oxidation of propane was studied; $LaSrCoO_4$ was shown to be the most active [8].

In the present paper we investigate the oxygen exchange and surface reactivity and discuss it in relation to the oxygen mobility in $La_{1-x}Sr_xCoO_{3-\delta}$ ($x = 0.0$, 0.3, 0.5) and layered $LaSrCoO_4$ and its correlation with the catalytic activity of these phases.

* Corresponding author.
E-mail address: mazo@inorg.chem.msu.ru (G. Mazo).

1293-2558/03/$ – see front matter © 2003 Éditions scientifiques et médicales Elsevier SAS. All rights reserved.
doi:10.1016/S1293-2558(03)00052-9

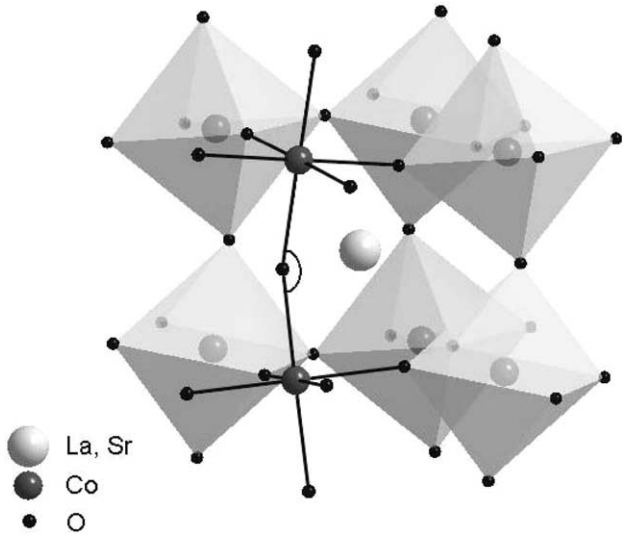

Fig. 1. Crystal structure of rhombohedrally distorted perovskite-type $La_{1-x}Sr_xCoO_{3-\delta}$ ($0 < x < 0.5$). Two octahedra are shown without faces to indicate their tilting.

2. Experimental section

2.1. Sample preparation

In order to ensure a large surface area, the freeze-drying method was used. Initial standardized nitrate solutions were mixed in the ratio corresponding to the compositions $La_{1-x}Sr_xCoO_{3-\delta}$ ($x = 0.0$, 0.3, 0.5) and $LaSrCoO_4$ and subjected to freeze-drying at $P = 5 \cdot 10^{-2}$ mbar followed by thermal decomposition performed by slow heating ($0.5° \text{ min}^{-1}$) in air up to 600 °C. Then, samples were annealed at 800 °C for 40 hours in air. As it has been demonstrated earlier [9,10], these conditions allow to obtain single phase La–Sr cobaltates.

2.2. Sample characterization

Samples were characterized by XRD in as-prepared state and after catalytic experiments using STADI P diffractometer (Cu $K_{\alpha 1}$ radiation). XR-diffraction using Guinier-de-Wolff camera (Cu $K_{\alpha 1}$ radiation, Ge as internal standard) was applied to calculate lattice parameters.

Specific surface areas were calculated via BET equation after degassing the samples at 300 °C and analyzing the N_2 adsorption isotherms at liquid nitrogen temperature using ASAP 2000 Micromeritics instrument.

Micromorphology and average particle size of powder samples was studied by scanning electron microscopy (JEM-2000FXII) ($U = 200$ kV).

The cation composition of the samples was controlled by energy-dispersive X-ray (EDX) analysis using a scanning electron microscope JEOL JSM-840A equipped with PGT IMIX system.

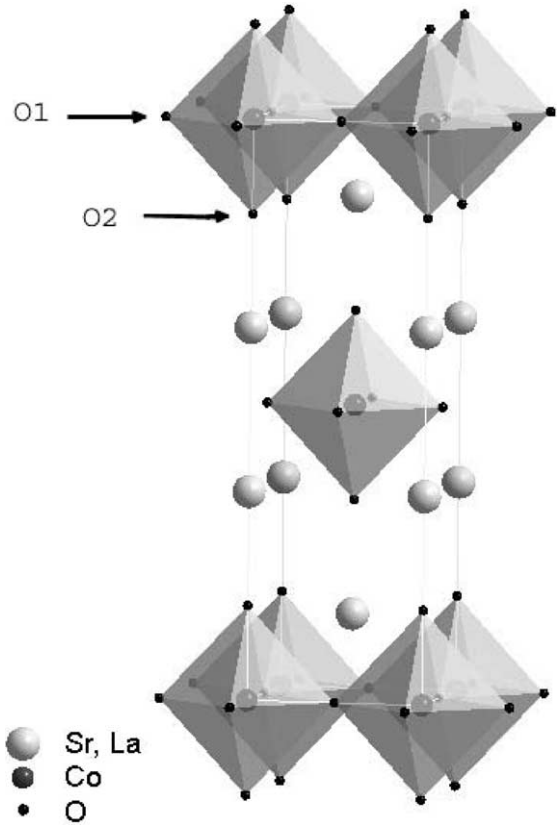

Fig. 2. Crystal structure of layered $La_{2-x}Sr_xCoO_{4\pm\delta}$ with tetragonal K_2NiF_4-type structure.

Iodometric titration was performed in order to determine the average cobalt oxidation state in as-prepared samples using the method similar to that described elsewhere [11].

2.3. Temperature programmed ^{18}O isotope exchange (TPIE) and CH_4 oxidation measurements

^{18}O exchange and CH_4 oxidation experiments were carried out in a quartz reactor with online-coupled mass spectrometer. Before starting the reaction approximately 200–600 mg of the sample, depending on surface area, was annealed for 4 hours at 400 °C in $^{16}O\,^{16}O$ flow (200 Pa), to remove adsorbed H_2O and CO_2 molecules from the solid surface. After cooling down to 100 °C, a mixture of Ar, $^{18}O\,^{18}O$ and second reactant ($^{16}O^{16}O$ or CH_4) in an appropriate ratio (1:4:4 for the exchange measurement and 1:4:2 for methane oxidation) was introduced. The pressure was adjusted to 120 Pa, then, the reactor was heated to 700 °C with a constant heating rate of $10° \text{ min}^{-1}$. The composition of the gas phase was analyzed by a quadrupole mass spectrometer. From the temperature dependence of ionic currents of different molecular forms in the gas phase the sequence of exchange, diffusion and oxidation processes was derived. The experimental error of temperature determination was ±5°.

Table 1
Lattice parameters, oxygen nonstoichiometry and BET surface area of the samples studied

Sample	Space group	Lattice parameters		Average cobalt oxidation state	δ	S_{BET}	Average particle size
		a (Å)	c (Å)			($m^2\,g^{-1}$)	(nm)
$LaCoO_{3-\delta}$	$R\bar{3}c$	5.445(1)	13.094(3)	2.98	0.01(2)	1.41(11)	300–350
$La_{0.7}Sr_{0.3}CoO_{3-\delta}$	$R\bar{3}c$	5.444(1)	13.208(4)	3.22	0.04(2)	1.87(12)	200–250
$La_{0.5}Sr_{0.5}CoO_{3-\delta}$	$R\bar{3}c$	5.430(1)	13.252(3)	3.34	0.08(2)	2.81(16)	100–150
$LaSrCoO_{4\pm\delta}$	$I4/mmm$	3.8020(6)	12.468(4)	3.00	0.00(2)	2.60(14)	100–150

2.4. Catalytic oxidation of CO and CH_4

The experiments on catalytic oxidation of CO and CH_4 were performed in an up-flow, fixed-bed quartz reactor. Approximately 500 mg of the sample powder was pressed in a pellet, then, crushed to obtain the catalyst in the granular form (granule size 0.5–1 mm). These samples were pretreated in N_2 flow for 1 hour at 450 °C. After cooling down, the sample was exposed to the reaction gas mixture. In CO oxidation experiments the starting temperature was 50 °C, and the reaction gas mixture consisted of CO (3.3 ml min^{-1}) and O_2 (3.3 ml min^{-1}). Methane oxidation measurements started at the $T = 250$ °C (CH_4, 1.4 ml min^{-1}, O_2, 5.2 ml min^{-1}). After 20 min of processing, the gas composition (at the outlet) was analyzed by online gas chromatograph (Shimadzu 17A) with thermal-conductivity detector. The conversion of CO and methane was calculated in terms of CO_2 formed.

3. Results

3.1. Sample preparation and characterization

After calcinations of freeze-dried salt precursors, black powders were obtained. According to XRD data, all samples were single-phase. Lattice parameters, average cobalt oxidation state and indices of oxygen nonstoichiometry (δ) calculated from the data of iodometric titration are given in the Table 1. The cation ratios La:Sr:Co according to EDX results for $LaCoO_{3-\delta}$, $La_{0.3}Sr_{0.7}CoO_{3-\delta}$, $La_{0.5}Sr_{0.5}CoO_{3-\delta}$ and $LaSrCoO_{4\pm\delta}$ are 52:0:48, 34:15:51, 27:24:49 and 35:33:32 at%, respectively. $La_{1-x}Sr_xCoO_{3-\delta}$ ($x = 0.0$, 0.3, 0.5) demonstrated rhombohedrally distorted perovskite structure, with increasing x the structure becomes less distorted, being in agreement with the data of Mineshige et al. [12] $LaSrCoO_{4\pm\delta}$ has tetragonal K_2NiF_4-type structure, which is a two-dimensional analogue of perovskite. Sr-doped perovskite cobaltates are oxygen deficient, unlike $LaCoO_3$ and $LaSrCoO_4$, which are nearly stoichiometric. BET surface areas of the samples (Table 1) are in the range of 1.3–3.0 $m^2\,g^{-1}$ and agree well with the values of the average particle size obtained from SEM images.

It is worth noting that after catalytic experiments and isotope exchange the samples remained single phase, no additional peaks could be observed in diffraction patterns.

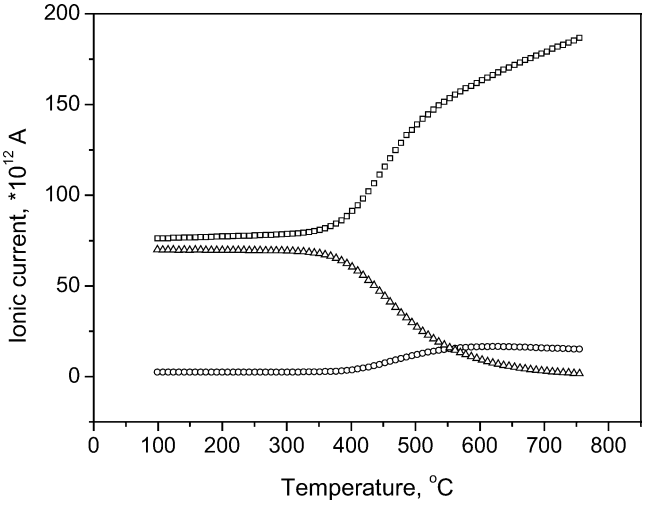

Fig. 3. Temperature dependence of ionic currents of all oxygen forms during the experiment over $LaSrCoO_{4.00}$ (□, $^{16}O\,^{16}O$; △, $^{18}O\,^{18}O$; ○, $^{18}O\,^{16}O$).

3.2. Temperature programmed ^{18}O isotope exchange

The experiments were carried out in such a way that all factors (pretreatment and experimental conditions, oxygen partial pressure, total pressure, temperature regime, catalyst surface area) affecting the reactivity of solid, were the same in order to ensure the correct comparison.

During the oxygen isotope exchange experiments, all types of oxygen molecules—$^{16}O\,^{16}O$, $^{16}O\,^{18}O$ and $^{18}O\,^{18}O$—can be formed in the gas phase. The typical temperature dependence of their ionic currents is shown at Fig. 3.

The following diffusion and exchange processes can be distinguished:

- *homomolecular exchange*:

$$^{16}O\,^{16}O_{(g)} + {}^{18}O\,^{18}O_{(g)} \rightarrow 2\,{}^{18}O\,^{16}O_{(g)}, \quad (1)$$

  which occurs on the surface of the solid without direct participation of lattice oxygen;
- *partially heteromolecular exchange*:

$$^{18}O\,^{18}O_{(g)} + {}^{16}O_{(s)} \rightarrow {}^{18}O\,^{16}O_{(g)} + {}^{18}O_{(s)}; \quad (2)$$

  one of the oxygen atoms is exchanged with surface oxygen of oxide catalyst;
- *completely heteromolecular exchange*:

$$^{18}O\,^{18}O_{(g)} + 2\,{}^{16}O_{(s)} \rightarrow {}^{16}O\,^{16}O_{(g)} + 2\,{}^{18}O_{(s)}; \quad (3)$$

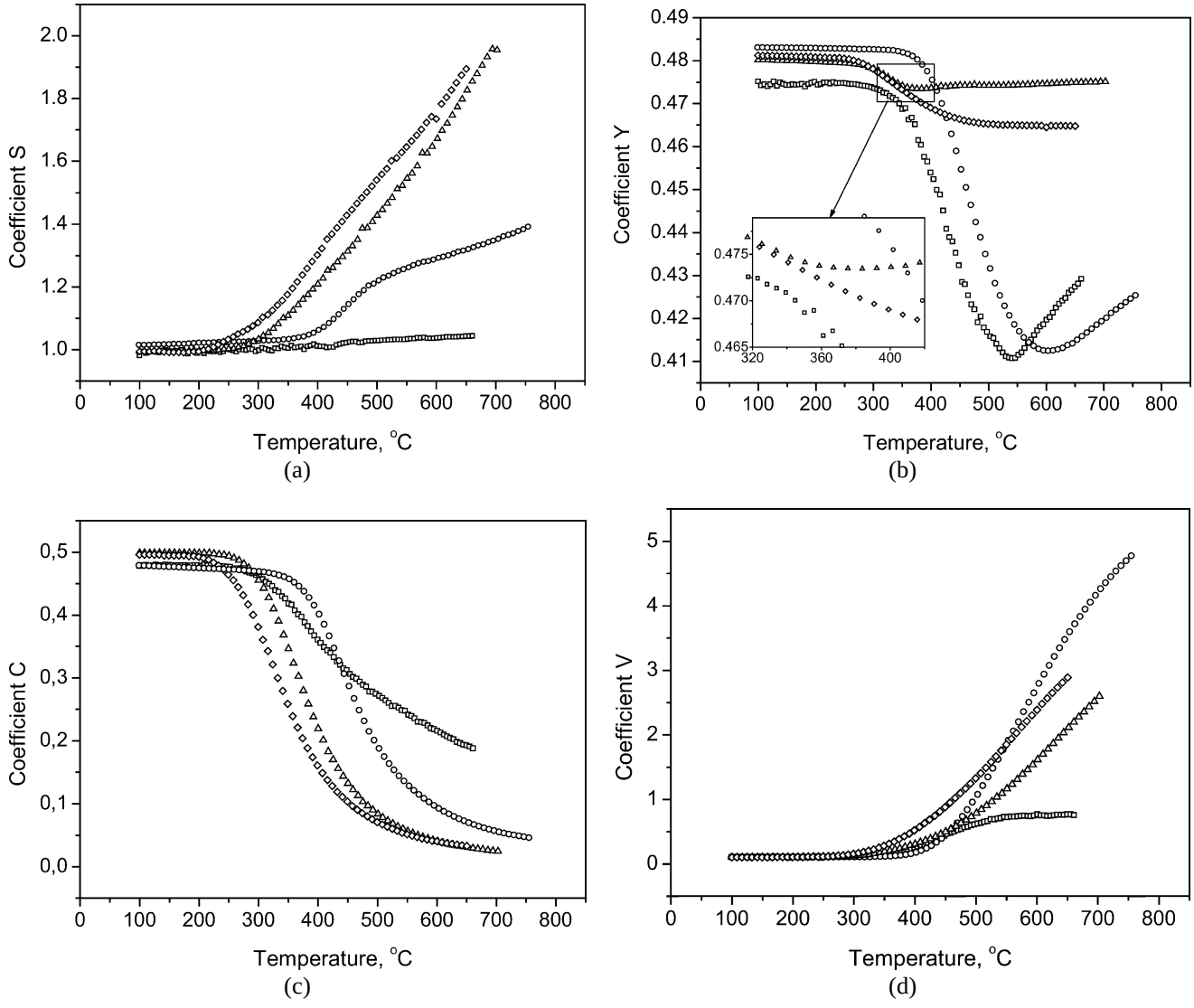

Fig. 4. Temperature-dependent variation of the isotope exchange coefficients: (a) coefficient S, (b) coefficient C, (c) coefficient Y, (d) coefficient V (□, $LaCoO_{2.99}$; △, $La_{0.7}Sr_{0.3}CoO_{2.96}$; ◇, $La_{0.5}Sr_{0.5}CoO_{2.92}$; ○, $LaSrCoO_{4.00}$).

both atoms of oxygen molecule are exchanged with surface oxygen of the solid;

- *out-diffusion*:

$$2^{16}O_{(s)} \rightarrow {}^{16}O\,{}^{16}O_{(g)}, \tag{4}$$

the release of oxygen from the solid. The process takes place, if the oxygen activity in the gas phase is lower than that in the oxide.

These processes may take place separately or simultaneously depending on both composition of the analyzed compound and temperature. However from the variation of the isotopic ratio in the phase it is difficult to conclude which reaction dominates in a certain temperature region. The isotope exchange coefficients were introduced [13,14] to choose dominating reaction between simultaneously occurring processes. The definition of all the coefficients is described in detail elsewhere [15]. Temperature dependencies of the mentioned coefficients are presented at Figs. 4a–4d.

The coefficient S corresponds to the change of oxygen partial pressure,

$$S = \frac{\{[{}^{16}O\,{}^{16}O] + [{}^{16}O\,{}^{18}O] + [{}^{18}O\,{}^{18}O]\}_t}{\{[{}^{16}O\,{}^{16}O] + [{}^{16}O\,{}^{18}O] + [{}^{18}O\,{}^{18}O]\}_{t_0}} = \frac{p}{p_0}, \tag{5}$$

it increases if out-diffusion takes place.

For oxygen deficient $La_{0.7}Sr_{0.3}CoO_{2.96}$ and $La_{0.5}Sr_{0.5}CoO_{2.92}$ the liberation of oxygen begins at lower temperatures (250 and 200 °C, respectively), than for $LaCoO_{2.99}$ and $LaSrCoO_{4.00}$ (Table 2), which initial oxygen content was close to stoichiometric.

The coefficient C characterizes the relative ^{18}O content in the gas phase,

$$C = \frac{[{}^{16}O\,{}^{18}O]/2 + [{}^{18}O\,{}^{18}O]}{[{}^{16}O\,{}^{16}O] + [{}^{16}O\,{}^{18}O] + [{}^{18}O\,{}^{18}O]}. \tag{6}$$

Table 2
Onset temperatures of isotope exchange, out-diffusion and methane oxidation by $^{18}O\,^{18}O$, °C

Sample	Completely heteromolecular exchange, T_{ex1}	Partially heteromolecular exchange, T_{ex2}	Homomolecular exchange	Out-diffusion, T_{diff}	Methane oxidation, T_{ox}
$LaCoO_{2.99}$	280	350	320	350	460
$La_{0.7}Sr_{0.3}CoO_{2.96}$	225	250	385	250	390
$La_{0.5}Sr_{0.5}CoO_{2.92}$	220	220	360	200	360
$LaSrCoO_{4.00}$	275	300	450	315	400

It decreases when release of oxygen or/and heteromolecular exchange occurs, while homomolecular exchange does not influence C.

For $La_{0.5}Sr_{0.5}CoO_{2.92}$ coefficients C and S begin to change at the same temperature. This means, that both release of oxygen or isotope exchange may occur, but it is difficult to distinguish these processes in this case. For all other samples in this study the onset temperature of diffusion T_{diff} (Table 2) is higher than the similar parameter for isotope exchange (T_{ex}) (Table 2).

Comparative analysis of S and C coefficients may be helpful in distinguishing out-diffusion and heteromolecular exchange, but the type of the dominating completely or partially heteromolecular exchange process cannot be determined from the C and S curves. Some information can be gained from the temperature dependence of ionic currents of oxygen molecules. From Fig. 3 it is seen that at $T = T_{ex1}$ the concentration of $^{16}O\,^{16}O$ becomes higher and the ionic current of $^{18}O\,^{18}O$ molecules decreases while the quantity of $^{18}O\,^{16}O$ in the gas phase remains unchanged until the temperature reaches T_{ex2} value. This indicates that completely heteromolecular exchange takes place in the temperature interval from T_{ex1} to T_{ex2}.

The coefficient Y can be introduced as a difference between relative $^{18}O\,^{16}O$ content in the state of equilibrium and at the time t:

$$Y = \left\{\frac{[^{18}O\,^{16}O]}{[^{16}O\,^{16}O] + [^{16}O\,^{18}O] + [^{18}O\,^{18}O]}\right\}_{eq} - \left\{\frac{[^{18}O\,^{16}O]}{[^{16}O\,^{16}O] + [^{16}O\,^{18}O] + [^{18}O\,^{18}O]}\right\}_{t}. \quad (7)$$

It describes the deviation of the isotopic composition of the gas phase from the equilibrium state. Y approaches zero if $^{18}O\,^{16}O$ is formed by isotope exchange reaction, and increases when out-diffusion is favored.

When temperature is higher than 520 °C, decrease of the relative concentration of $^{18}O\,^{16}O$, resulting from out-diffusion for $La_{0.5}Sr_{0.5}CoO_{2.92}$, is compensated by its increase due to isotope exchange, so that the value of Y remains constant. All other studied compounds demonstrated an increase of Y with onset temperatures of 380, 550 and 605 °C for $La_{0.7}Sr_{0.3}CoO_{2.96}$, $LaCoO_{2.99}$ and $LaSrCoO_{4.00}$, respectively. It is worth mentioning that for $LaCoO_{2.99}$ and $LaSrCoO_{4.00}$ the isotope exchange is more intensive and lower values of Y coefficient for these compounds demonstrate lower difference between actual and equilibrium compositions of the gas phase.

Appearance of $^{18}O\,^{16}O$ in the gas phase may result from occurrence of either partially heteromolecular or homomolecular exchange. The V coefficient can help to distinguish between those processes. The V coefficient is a measure of the $^{18}O\,^{16}O$ partial pressure related to the sum of ^{18}O containing oxygen molecules:

$$V = \left\{\frac{[^{16}O\,^{18}O]/2}{[^{16}O\,^{18}O]/2 + [^{18}O\,^{18}O]}\right\}_{t} \times \left\{\frac{[^{16}O\,^{18}O]/2 + [^{18}O\,^{18}O]}{[^{16}O\,^{18}O]/2}\right\}_{t_0}. \quad (8)$$

As can be seen from Eq. (8), the value of V coefficient is independent on the $^{16}O\,^{16}O$ content. This parameter changes during various exchange reactions (Eqs. (1)–(3)) but it is insensitive to the diffusion process (Eq. (4)).

The comparison of experimental data, obtained in the environment with various oxygen isotopes ratio, allows to obtain the information about the limiting stage of isotope exchange process. For the calculation of V values we used the data of two experiments. In the first case we studied the catalytic methane oxidation using only $^{18}O\,^{18}O$ (curve 1 at Fig. 5 for $LaSrCoO_{4.00}$). Curve 2 at Fig. 5 is obtained for isotope exchange reaction at the same conditions, when both $^{16}O\,^{16}O$ and $^{18}O\,^{18}O$ isotopes were present in the gas phase. In the first case the reaction of homomolecular exchange (Eq. (3)) can appear only in the case of ^{16}O out-diffusion from the sample.

For both methane oxidation and isotope exchange reactions (curves 1 and 2, Fig. 5) the values of V increase starting at 275 °C, which shows the occurrence of exchange reactions. At the same temperature, the decrease of C coefficient (Fig. 4b), related to the heteromolecular exchange, is observed, so that the increase of V values should be attributed to the heteromolecular exchange (Eqs. (2), (3)). Different behavior of curves 1 and 2 between 450 and 750 °C is attributed to homomolecular exchange with $^{16}O\,^{16}O$ of the gas phase. For the $LaCoO_{2.99}$, $La_{0.7}Sr_{0.3}CoO_{2.96}$ and $La_{0.5}Sr_{0.5}CoO_{2.92}$, homomolecular exchange process is observed at the temperature 320, 385 and 360 °C, respectively.

3.3. Catalytic combustion of CO

The oxidation of carbon monoxide was investigated under dynamic conditions (Fig. 6). The temperature of 5%

Table 3
Light-off temperatures and activation energies of CH_4 and CO oxidation

Sample	Average cobalt oxidation state	CH_4 oxidation		CO oxidation	
		Light-off temperature (°C)	Activation energy ($kJ\,mol^{-1}$)	Light-off temperature (°C)	Activation energy, ($kJ\,mol^{-1}$)
$La_{0.7}Sr_{0.3}CoO_{2.96}$	3.22	330	25(7)	120	8(3)
$La_{0.5}Sr_{0.5}CoO_{2.92}$	3.34	325	23(7)	150	5(2)
$LaSrCoO_{4.00}$	3.00	375	27(8)	185	9(4)

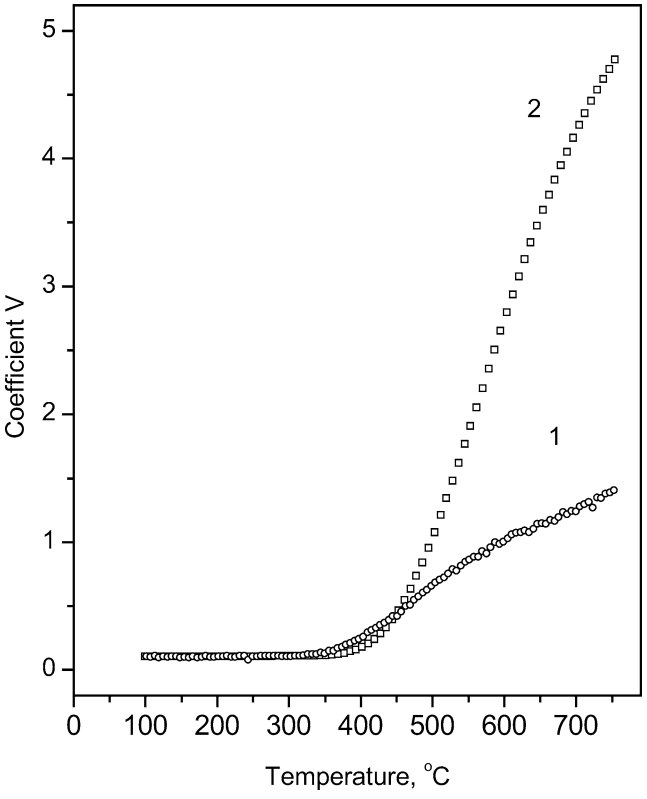

Fig. 5. Temperature dependence of coefficient V for $LaSrCoO_{4.00}$ under different experimental conditions: ○, calculated from the data of the methane oxidation experiment without $^{16}O^{16}O$ in the gas phase at the beginning of the experiment (curve 1); □, calculated from the data of the isotope exchange experiment with $^{16}O\,^{16}O$ and $^{18}O\,^{18}O$ in the gas phase (curve 2).

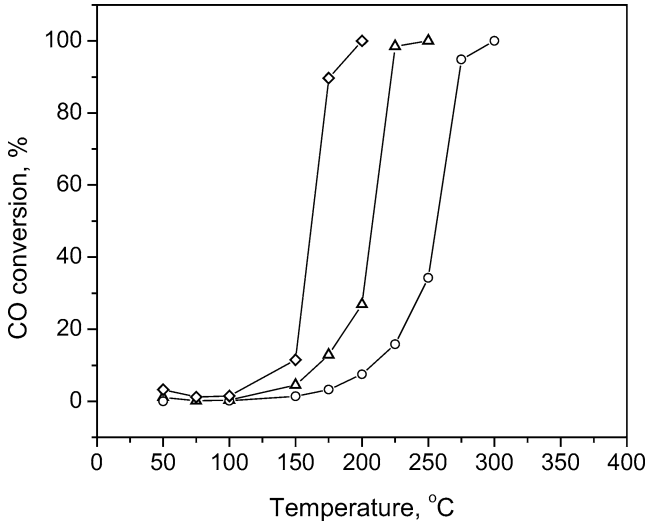

Fig. 6. Light-off temperature curves for oxidation of carbon monoxide over (△) $La_{0.7}Sr_{0.3}CoO_{2.96}$, (◇) $La_{0.5}Sr_{0.5}CoO_{2.92}$, (○) $LaSrCoO_{4.00}$.

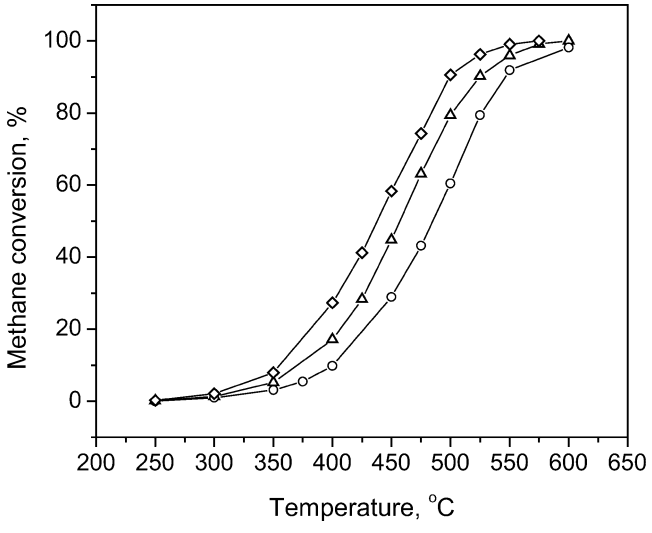

Fig. 7. Light-off temperature curves for methane oxidation over (△) $La_{0.7}Sr_{0.3}CoO_{2.96}$, (◇) $La_{0.5}Sr_{0.5}CoO_{2.92}$, (○) $LaSrCoO_{4.00}$.

conversion is referred to as light-off temperature (Table 3). The activation energies were evaluated using the method described elsewhere [16]. These values can be used as the qualitative characteristic of the samples, as the mechanism of the oxidation process cannot be exactly determined in this case.

3.4. Catalytic combustion of CH_4

In order to obtain detailed information on the role of oxygen in methane oxidation mechanism, several experiments on the catalytic oxidation of methane under dynamic conditions (Fig. 7) and with $^{18}O\,^{18}O$ (Figs. 8, 9) have been also performed.

The experiments on CH_4 oxidation by $^{18}O\,^{18}O$ were carried out under conditions similar to isotope exchange studies. No $^{16}O\,^{16}O$ oxygen was detected at the beginning of the experiments. Decrease of CH^{3+} ionic current (Fig. 8) and appearance of CO_2 in the gas phase (Fig. 9) indicate the beginning of oxidation. It should be noted, that no CO_2 (48 AMU) is formed during the oxidation process. Two ways

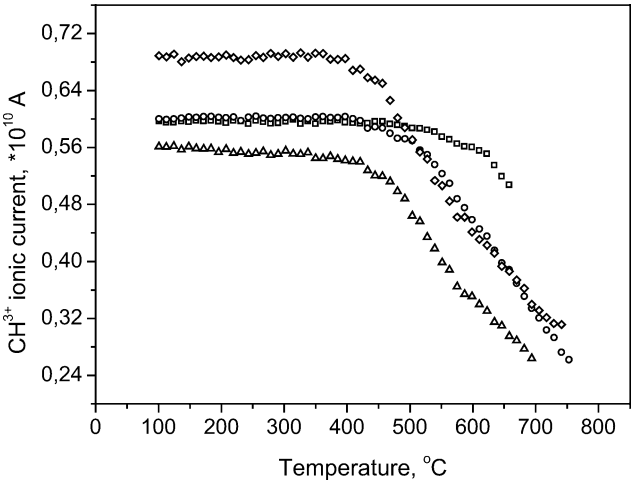

Fig. 8. Temperature dependence of CH^{3+} ionic current in the methane oxidation experiments (□, $LaCoO_{2.99}$; △, $La_{0.7}Sr_{0.3}CoO_{2.96}$; ◇, $La_{0.5}Sr_{0.5}CoO_{2.92}$; ○, $LaSrCoO_{4.00}$).

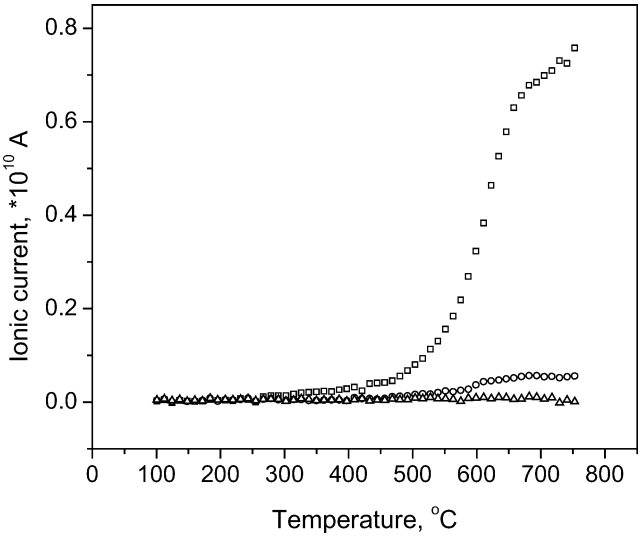

Fig. 9. Typical dependence of ionic currents of different forms of CO_2 in the methane oxidation experiments. The experimental curves for $LaSrCoO_{4.00}$ are given as an example (□, CO_2 (44 AMU); ○, CO_2 (46 AMU); △, CO_2 (48 AMU)).

of CO_2 (46 AMU) formation are possible: either isotope exchange between $C^{16}O^{16}O$ and $^{18}O\,^{18}O$ ($^{18}O\,^{16}O$) occurs or some ^{18}O is present at the surface of the catalyst at the moment of starting the oxidation reaction. Obviously, ^{16}O from the solid acts as oxidizing agent. Thus, oxygen mobility seems to be the crucial factor in these catalytic processes. It can be illustrated by the data of Table 2: strong correlation between onset temperatures of the isotope exchange (T_{ex}), oxidation (T_{ox}) and out-diffusion processes is observed.

4. Discussion

4.1. Oxygen mobility

For perovskites $La_{1-x}Sr_xCoO_{3-\delta}$ the onset temperatures of heteromolecular exchange become lower as Sr content increases. This occurs due to the formation of vacancies in the oxygen sublattice as a result of heterovalent doping. $LaCoO_{2.99}$ has less deficient oxygen sublattice and, hence, the lowest oxygen mobility in the row of perovskite-type cobaltates. On the other hand, the average oxidation state of cobalt increases with strontium doping, and oxygen atoms should be stronger bonded in the structure. The correlation of the onset temperatures of out-diffusion (T_{diff}) (Table 2) with initial oxygen nonstoichiometry ($\delta = 0.01(2)$, 0.04(2), 0.08(2) for $x = 0.0$, 0.3, 0.5, respectively) also indicates the major role of oxygen vacancy concentration.

Layered $LaSrCoO_{4.00}$ with stoichiometric oxygen content shows higher oxygen mobility in comparison with $LaCoO_{2.99}$, though both phases have cobalt in the 3+ oxidation state. Increase of S coefficient, responsible for oxygen partial pressure change during the whole temperature region studied, is less than 10% for $LaCoO_{2.99}$ because of the low concentration of oxygen vacancies. On the contrary, the S coefficient shows an interesting behavior for $LaSrCoO_{4.00}$ when the temperature is raised. The regions with different oxygen release rate are clearly seen in Fig. 4a. In the first interval ($300 < T < 350\,^{\circ}C$) the oxygen out-diffusion starts, then at $350 < T < 500\,^{\circ}C$, oxygen release is rather intensive; and, finally when temperature is higher than 500 °C, the process occurs at lower rate. It may be related to two kinds of oxygen sites present in this structure. First, weakly bonded oxygen is eliminated providing vacancies for the oxygen atoms of the second type involved in diffusion to move through. Such effect was not observed by Nitadory et al. [8] using TPD method. The comparison of oxygen mobility of perovskite and layered structured phases with equal cobalt oxidation states and deficiency of oxygen sublattice allows to expect higher mobility of oxygen in $La_{2-x}Sr_xCoO_{4-\delta}$ with $x > 1$.

4.2. Oxidation of carbon monoxide

All studied compounds catalyze CO oxidation, full conversion is achieved at 200, 250 and 300 °C for $La_{0.5}Sr_{0.5}CoO_{3-\delta}$, $La_{0.7}Sr_{0.3}CoO_{3-\delta}$ and $LaSrCoO_{4.00}$, respectively. The activation energies are rather low (Table 3) and the values are nearly the same within experimental error.

Concerning the mechanism, the oxidation of carbon monoxide has been considered as so-called *suprafacial* [1] catalytic process, where the structure and the properties of surface seem to be very important. The following mechanism of CO oxidation on $LaCoO_3$ was proposed by Tascon et al. [17]:

$$O_{2(g)} \rightarrow O_{2(ads)} \rightarrow 2O_{(ads)}$$

$CO_{(g)} \rightarrow CO_{(ads)}$

$CO_{(ads)} + 2O_{(ads)} \rightarrow CO_{3(ads)}$

$CO_{3(ads)} \rightarrow CO_{2(ads)} + O_{(ads)}$

$CO_{2(ads)} \rightarrow CO_{2(g)}$

The authors suggested, that La^{3+} ions are catalytically inactive, whereas cobalt and oxygen ions act as adsorption and activation centers for O_2 and CO, respectively. Adsorbed atomic oxygen and CO interact, producing $CO_{3(ads)}$, that decomposes later yielding CO_2 and oxygen. It was previously observed that activity of perovskites in CO oxidation depends on the electronic configuration of the transition metal ion. The maximum activity is observed when occupancy of e_g levels is less than one electron, while t_{2g} levels are half- or totally filled [4].

In case of cobaltates studied here the average oxidation state of cobalt is between 3+ and 4+ (Table 3). The trivalent cobalt in perovskite structure (d^6 configuration) can present in low-spin Co^{3+} ($t_{2g}^6 e_g^0$) or high-spin Co^{3+} ($t_{2g}^4 e_g^2$) state. The former is preferred at low temperatures (below 100 K), the latter—at higher temperatures (above 1000 K), in the middle temperature range high-spin and low-spin can coexist [18,19], the intermediate-spin state ($t_{2g}^5 e_g^1$) was also stated for trivalent cobalt ions [20]. Tetravalent cobalt ions are present in low-spin state Co^{4+} ($t_{2g}^5 e_g^0$) [18]. In layered $La_{2-x}Sr_xCoO_4$ structure trivalent cobalt was supposed to have intermediate-spin state, if $x \geqslant 0.8$ [21]. Thus the activity of cobaltates in CO oxidation (Fig. 6) is in line with observations of Tascon et al. [4].

The highest activity of $La_{0.5}Sr_{0.5}CoO_{3-\delta}$ in CO oxidation is probably explained by the fact, that rhombohedral distortion of the structure (Fig. 1) decreases with increase of x up to $x = 0.5$. The closer the structure to the cubic (Co–O–Co angle is equal to 180°), the easier is electron exchange between Co^{4+} and Co^{3+} through the p-orbital of oxygen: Co^{3+}–O^{2-}–$Co^{4+} \longleftrightarrow Co^{4+}$–$O^{2-}$–$Co^{3+}$.

4.3. Mechanistic aspects of methane oxidation

It is supposed, that the mechanism of methane oxidation changes with temperature. According to the terminology used in catalysis [3], the reaction is *suprafacial* at low temperatures and *intrafacial* (surface atoms of the catalyst are involved in catalytic action) at higher temperatures [1–3]. The defect structure is considered to be the controlling factor at high temperatures.

The experimental results discussed above clearly show that starting from the temperature T_{ox} the reaction mechanism under the conditions used should be considered as intrafacial. It contradicts the data of Arai et al. [22], where participating both—adsorbed from the gas phase and lattice—kinds of oxygen in the reaction was stated in the temperature range 450–650 °C. Although the reaction order for methane and oxygen cannot be calculated in this case, the absence of $C\,^{18}O\,^{18}O$ and the catalytic activity dependence on the defects concentration in the structure indicates that the reaction rate is controlled by the mobility of the lattice oxygen. The following speculative mechanism of the oxidation reaction can be derived:

$CH_4 \longleftrightarrow CH_{4(ads)}$

$2O^{2-} + CH_{4(ads)} \rightarrow CO_2 + 8e^- + 4H^+$

$2O^{2-} + 4H^+ \rightarrow 2H_2O$

$8Co^{4+} + 8e^- \rightarrow 8Co^{3+}$ (or $8Co^{3+} + 8e^- \rightarrow 8Co^{2+}$)

$8Co^{3+} + 2O_2 \rightarrow 8Co^{4+} + 4O^{2-}$

(or $8Co^{2+} + 2O_2 \rightarrow 8Co^{3+} + 4O^{2-}$)

First, methane and $^{18}O\,^{18}O$ adsorb on the catalyst surface. Then $^{16}O^{2-}$ from the bulk reduces Co^{4+} from the surface layer to Co^{3+} (or Co^{3+} to Co^{2+}) and forms active oxygen to oxidize CH_4 to CO_2. ^{18}O from the surface oxidizes Co^{3+} to Co^{4+} (or Co^{2+} to Co^{3+}) and incorporates into the lattice as $^{18}O^{2-}$. The presence of vacancies in the catalyst lattice facilitates the diffusion of $^{18}O^{2-}$ from the surface into the bulk of the catalyst, and diffusion of $^{16}O^{2-}$ from the bulk to the surface, enhancing the catalytic activity.

5. Conclusions

The results of ^{18}O-isotope exchange experiments and data of the methane oxidation by $^{18}O\,^{18}O$ gas enabled to establish the correlation between initial oxygen deficiency of catalyst, oxygen mobility in solid phase and catalytic activity of the materials, based on complex cobaltates. Identical experimental conditions for all samples allowed us to exclude all factors influencing the catalytic process except the composition of the catalyst. It should be noted that catalytic activity in methane oxidation is determined by the mobility of oxygen ions in the structure. Oxygen deficiency of the sublattice is a more important factor than the oxidation state of cobalt. The reaction occurs via intrafacial mechanism; reaction steps are specified. On the example of $LaSrCoO_4$ we have shown, that layered cobaltates are, probably, more active in catalysis and exchange processes compared to other perovskites with the same oxygen stoichiometry and cobalt oxidation state. Layered cobaltates with strontium doping ratio higher than 1 seem to be more active in the oxidation processes controlled by mobile lattice oxygen. Additional studies have to be performed to verify this hypothesis.

Acknowledgements

The work was supported by Russian Foundation for Basic Research through Grant No. 00-03-32356a. L.B. is obliged to the Deutscher Akademischer Austauschdienst for the Leonard Euler stipendium.

References

[1] R.J.H. Voorhoeve, J.P. Remeika, L.E. Tribble, Ann. N.Y. Acad. Sci. 272 (1976) 3.
[2] M.A. Pena, J.L.G. Fierro, Chem. Rev. 101 (2001) 1981.
[3] L.G. Tejuca, J.L.G. Fierro, J.M.D. Tascon, Adv. Catal. 36 (1989) 237, and references therein.
[4] J.M.D. Tascon, L.G. Tejuca, Reac. Kinet. Catal. Lett. 15 (1980) 185.
[5] T. Nakamura, M. Misono, Y. Yoneda, Bull. Chem. Soc. Jpn. 55 (1982) 394.
[6] T. Nakamura, M. Misono, Y. Yoneda, J. Catal. 83 (1983) 151.
[7] I.D. Brown, D. Altermatt, Acta Cryst. B 41 (1985) 224.
[8] T. Nitadori, M. Muramatsu, M. Misono, Chem. Mater. 1 (1989) 215.
[9] I.A. Koudriashov, L.V. Borovskikh, G.N. Mazo, S. Scheurell, E. Kemnitz, Magnetoresistive Oxides and Related Materials, in: M. Rzchowski, et al. (Eds.), MRS Fall Meeting Proceedings 602 (1999) 377.
[10] L.V. Borovskikh, G.N. Mazo, O.A. Shlyakhtin, 8th European Conference on Solid State Chemistry, Oslo, Norway, 3–7 July 2001, Book of Abstracts P146.
[11] L.V. Borovskikh, G.N. Mazo, V.M. Ivanov, Vestnik Mosk. Univ., Khimiya 40 (1999) 373.
[12] A. Mineshige, M. Kobune, S. Fujii, Z. Ogumi, M. Inaba, T. Yao, K. Kekuchi, J. Solid State Chem. 142 (1999) 374.
[13] V.S. Muzikantov, V.V. Popovski, G.K. Boreskov, Kinet. Katal. 5 (1964) 624.
[14] A.A. Galkin, G.N. Mazo, S. Scheurell, E. Kemnitz, Solid Sate Ionics 101–103 (1997) 1087.
[15] E. Kemnitz, A.A. Galkin, T. Olesch, S. Scheurell, A.P. Mozhaev, G.N. Mazo, J. Therm. Anal. 48 (1997) 997.
[16] N. Gunasekaran, S. Saddawi, J.J. Carberry, J. Catal. 159 (1996) 107.
[17] J.M.D. Tascon, J.L.G. Fierro, L.G. Tejuca, Z. Phys. Chem. (Wiesbaden) 124 (1981) 249.
[18] P.M. Raccah, J.B. Goodenough, Phys. Rev. 155 (1967) 932.
[19] V.G. Bhide, D.S. Rajoria, G.R. Rao, C.N.R. Rao, Phys. Rev. B 6 (1972) 1021.
[20] G. Thornton, B.C. Tofield, D.E. Williams, Solid State Commun. 44 (1982) 1213.
[21] Y. Morimoto, K. Higashi, K. Matsuda, A. Nakamura, Phys. Rev. B 55 (1997) R14725.
[22] H. Arai, T. Yamada, K. Eguchi, T. Seiyama, Applied Catalysis 26 (1986) 265.